

University of Nebraska - Lincoln
DigitalCommons@University of Nebraska - Lincoln

Peter Dowben Publications

Research Papers in Physics and Astronomy

2013

Adsorption of TCNQH-functionalized quinonoid zwitterions on gold and graphene: evidence for dominant intermolecular interactions+

Lingmei Kong
University of Nebraska-Lincoln

Lucie Routaboul
Universite' de Strasbourg


Pierre Braunstein
Universite' de Strasbourg

Hong-Gi Park
Kyung Hee University

Jaewu Choi
Kyung Hee University, jchoi@ece.eng.wayne.edu

See next page for additional authors

Follow this and additional works at: <http://digitalcommons.unl.edu/physicsdowben>

 Part of the [Atomic, Molecular and Optical Physics Commons](#), [Condensed Matter Physics Commons](#), [Engineering Physics Commons](#), and the [Other Physics Commons](#)

Kong, Lingmei; Routaboul, Lucie; Braunstein, Pierre; Park, Hong-Gi; Choi, Jaewu; Colon Cordova, John P.; Vega, E; Rosa, Luis G.; Doudin, Bernard; and Dowben, Peter A., "Adsorption of TCNQH-functionalized quinonoid zwitterions on gold and graphene: evidence for dominant intermolecular interactions+" (2013). *Peter Dowben Publications*. 267.
<http://digitalcommons.unl.edu/physicsdowben/267>

This Article is brought to you for free and open access by the Research Papers in Physics and Astronomy at DigitalCommons@University of Nebraska - Lincoln. It has been accepted for inclusion in Peter Dowben Publications by an authorized administrator of DigitalCommons@University of Nebraska - Lincoln.

Authors

Lingmei Kong, Lucie Routaboul, Pierre Braunstein, Hong-Gi Park, Jaewu Choi, John P. Colon Cordova, E Vega, Luis G. Rosa, Bernard Doudin, and Peter A. Dowben

Adsorption of TCNQH-functionalized quinonoid zwitterions on gold and graphene: evidence for dominant intermolecular interactions†

Cite this: *RSC Advances*, 2013, 3, 10956

Lingmei Kong,^a Lucie Routaboul,^b Pierre Braunstein,^b Hong-Gi Park,^c Jaewu Choi,^c John P. Colón Córdova,^{ad} E. Vega,^{ad} Luis G. Rosa,^d Bernard Doudin^e and Peter A. Dowben^{*a}

We experimentally investigate the electronic structure of the strongly dipolar, quinonoid-type molecule obtained by TCNQH-functionalization (TCNQH = (NC)₂CC₆H₄CH(CN)₂) of (6Z)-4-(butylamino)-6-(butylimino)-3-oxocyclohexa-1,4-dien-1-olate C₆H₂(=NHR)₂(=O)₂ (where R = *n*-C₄H₉) to be very similar after deposition from solution on either graphene or gold substrates. These zwitterion adsorbate thin films form structures that are distinct from those formed by related quinonoid molecules previously studied. We argue that adsorbate–adsorbate interactions dominate and lead to a Stranski–Krastanov ‘island growth’ mechanism.

Received 22nd February 2013,
Accepted 2nd May 2013

DOI: 10.1039/c3ra40930a

www.rsc.org/advances

Introduction

A number of *p*-benzoquinoneminoimine zwitterion adsorbate thin films have now been investigated, using deposition from solution^{1–6} or from the vapour phase.^{6,7} These molecules were used as a model system for surface adsorption studies, taking advantage of their significant dipole moment of *ca.* 10 Debyes across a short distance, in order to gain a better insight into electrostatic contributions to surface adsorption phenomena. The chemical modification of the pendant groups attached to the nitrogen atoms (Fig. 1) also makes possible comparative studies of molecular thin films adsorption.² In general, there is pronounced adlayer ordering, with a variety of molecular orientations and packing arrangements from upright^{1,2} to lying flat^{5–7} that depend on both the method of deposition and the substrate, owing to varying adsorbate–substrate interactions.⁵

Chemical modifications of the *p*-benzoquinoneminoimine zwitterions (see graphical abstract and the molecules of Fig. 1)

used in adsorbate thin films can lead to supramolecular assemblies^{2,6,8} (like that observed for tetracyanoquinodimethane (TCNQ))^{9–16} and possibly better hole–electron charge separation. The latter could significantly influence the exciton recombination rate, a key issue in organic solar cell optimization, and reports illustrate how the addition of dipolar molecules improves solar cell efficiencies.^{17–20}

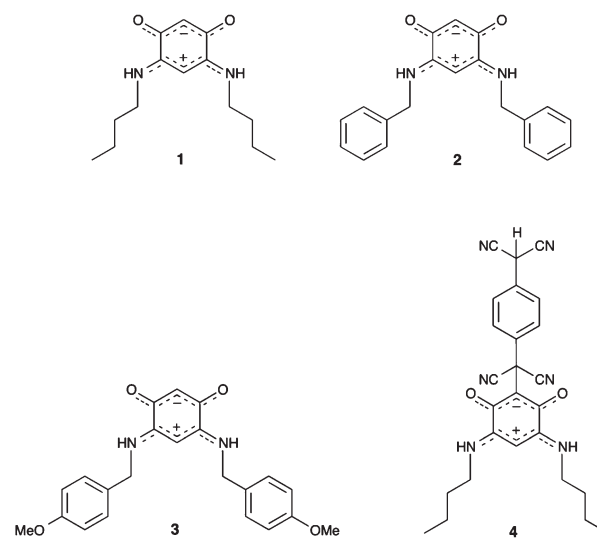


Fig. 1 The *p*-benzoquinoneminoimine zwitterions studied, including the dibutyl **1**, the dibenzyl **2**, the di(methoxybenzyl) **3**, and the TCNQ-derived *p*-benzoquinoneminoimine zwitterion **4**.

^aDept. of Physics and Astronomy and the Nebraska Center for Materials and Nanoscience, Univ. of Nebraska-Lincoln, Nebraska 68588-0299, USA.

E-mail: pdowben@unl.edu

^bLaboratoire de Chimie de Coordination, Institut de Chimie (UMR 7177 CNRS), Université de Strasbourg, 4 rue Blaise Pascal, 67081 Strasbourg, France

^cDept. of Information Display, Kyung Hee University, 1 Hoegi-dong, Dondaemoon-gu, Seoul 130-701, Korea

^dDept. of Physics and Electronics, University of Puerto Rico-Humacao, 100 Road 908 CUH Station, Humacao, PR, 00791, USA

^eInstitut de Physique et Chimie des Matériaux de Strasbourg, IPCMS (UMR 7504), and Laboratory of Nanostructures in Interactions with their Environment (NIE), Université de Strasbourg, 23 rue du Læss, B. P. 43, 67034 Strasbourg, France

† Electronic supplementary information (ESI) available. See DOI: 10.1039/c3ra40930a

Charge-assisted hydrogen bonding, which involves Coulombic interactions, is exceptionally appealing for molecular assembly and accounts *e.g.* for the remarkable properties of the charge transfer salts TTF (tetrathiofulvalene)–TCNQ (7,7,8,8-tetracyanoquinodimethane)^{21–26} and of the Bechgaard salts.^{25–29} It appeared to us attractive to functionalize the *p*-benzoquinonemonoimine zwitterion core by reaction with tetracyanoquinodimethane (TCNQ), which is one of the most widely used electron acceptors in organic solar cells. Adsorption of TCNQ and its derivatives on graphene and various metals has been widely studied,^{14–16,30–38} because of the presence of the four strongly electron-acceptor cyano groups with high electron affinity.^{38,39} For TCNQ, a *p*-doping of graphene results from a charge transfer of about 0.03 electron per C atom of graphene to the TCNQ adlayer.³⁴ Furthermore, both theoretical and experimental analyses successfully showed that F4-TCNQ (*i.e.* tetrafluoro TCNQ) can open a band gap and induce *p*-type doping on graphene, with both the doping level and magnitude of the band gap being controlled by the thickness of the F4-TCNQ adsorbed layer.^{33,40–43}

Here we present experimental surface (spectroscopy) studies of TCNQH-functionalized *p*-benzoquinonemonoimine zwitterions aimed at investigating adlayers on graphene, using adsorption on Au for comparison. We show that these molecular films have properties distinct from those obtained with previously studied quinonoid zwitterions, with intermolecular interactions being stronger than the molecule-substrate interactions.

Experimental methods

The functionalized *p*-benzoquinonemonoimine zwitterions **1–3** were synthesized according to established procedures.^{4,44,45} The *N*-butyl-substituted zwitterion (6*Z*)-4-(butylamino)-6-(butyliminio)-3-oxocyclohexa-1,4-dien-1-olate $C_6H_2(\equiv NHR)_2(\equiv O)_2$ (where R = *n*-C₄H₉) (**1** in Fig. 1), was functionalized, as described before, by chemoselective insertion of TCNQ into the C–H bond of the O=C=CH=C=O moiety to give **4** with the moiety (NC)₂CC₆H₄CH(CN)₂ as the C-substituent.^{46–48} Graphene was grown on copper foil by Chemical Vapor Deposition (CVD) at 1000 °C, at the pressure of 1.4 Torr for 30 min using the gas mixture of C₂H₂ (1.4 sccm) and H₂ (2 sccm). The zwitterions were deposited on clean gold and graphene substrates from a CH₂Cl₂ solution, as noted in prior work.^{1,2,4}

Combined photoemission (UPS) and inverse photoemission (IPES) studies were performed on molecules deposited on gold or graphene. The spectra were taken in a single ultrahigh vacuum chamber to study the placement of both occupied and unoccupied molecular orbitals of the quinonoid zwitterion, as was done in prior work.^{1,2,4} Experiments were performed with the electron emission (photoemission) or electron incidence (inverse photoemission) along the surface normal to preserve the highest symmetry. In both cases, the binding energies are

referenced to the Fermi edge of gold or copper, as appropriate, and the data are expressed in terms of $E - E_F$ (thus making occupied state energies negative). Film thickness and film uniformity were determined using atomic force microscopy (AFM) and core level X-ray photoemission (XPS), as in prior work with various adsorbed *p*-benzoquinonemonoimine zwitterions.²

Modeling

Calculations of the occupied and unoccupied molecular orbitals of molecular films were performed for comparison purposes with the density of states deduced from the UPS-IPES experiments. As in previous studies,^{1–4} the orbital energies of the single molecules (as in a gas phase experiment) were calculated using the neglect of differential overlap NDO-PM3 (neglect of differential overlap, parametric model number 3) based on Hartree–Fock formalism. Geometry optimization for each of the zwitterions was performed by obtaining the lowest restricted Hartree–Fock energy states. The density of states (DOS) were modelled by applying equal Gaussian envelopes of 1 eV full width half-maximum to each molecular orbital, to account for the solid-state broadening in photoemission, and then summing over each Eigen state. This model density of states calculations were rigidly shifted in energy, largely to account for the influence of the work function on the orbital energies and no correction was made for molecular interactions and final state effects. This is schematically indicated in Fig. 2, where the molecular orbital offsets are schematically illustrated for the methoxybenzyl-functionalized zwitterion $C_6H_2(\equiv NHR)_2(\equiv O)_2$, where R = –CH₂–C₆H₄–OCH₃ (**3** in Fig. 1) relative to the single molecule orbital calculations calculated by PM3 and the density functional theory (DFT). No correction was made for matrix element effects or light polarization and comparison with experiment requires caution as both photoemission and inverse photoemission are final state spectroscopies and the eigenvalues are from a ground state calculation.

Results

The methoxybenzyl-functionalized zwitterion $C_6H_2(\equiv NHR)_2(\equiv O)_2$, where R = –CH₂–C₆H₄–OCH₃ (schematically shown as **3** in Fig. 1), shows a significantly different placement of the lowest unoccupied molecular orbital (LUMO) when absorbed on gold (Fig. 3a) *versus* graphene (Fig. 3b), as previously observed for other *p*-benzoquinonemonoimine zwitterions.⁴ The energy states of the conduction band edge, related to the LUMO, are placed much closer to the Fermi level for **3** deposited on gold than on graphene (Fig. 3). The placement of unoccupied molecular orbitals for **3** on graphene is in reasonable agreement with expectations from the ground state single molecule orbital energies based on the semiempirical PM3 methodology (Fig. 2b and 3c). For **3** deposited on gold, a much better agreement is obtained with model ground

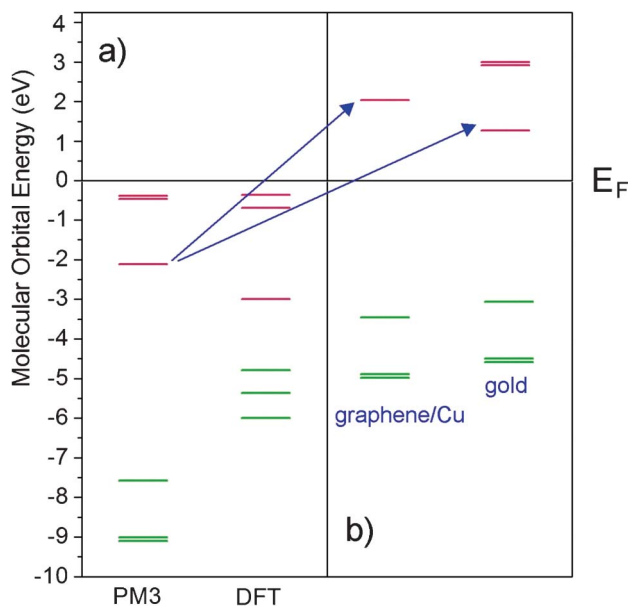


Fig. 2 Comparison of the lowest unoccupied molecular orbitals (red) and highest unoccupied molecular orbitals (green) orbital energies from single molecule semi-empirical PM3 and *ab initio* DFT calculations of the methoxybenzyl-functionalized zwitterion **3** (a) compared orbital energies for the molecular films on graphene on copper and on gold (b) now referenced to the substrate Fermi levels. Arrows indicate the experimentally determined molecular orbital offsets of the lowest unoccupied molecular orbital.

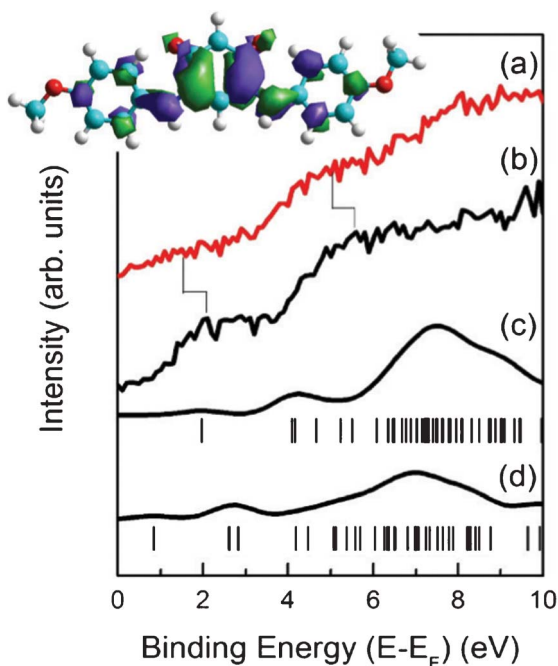


Fig. 3 The inverse photoemission spectra of **3** on Au (a) and graphene/Cu (b), along with the model calculation of the single molecule density of states, using a semi-empirical approach PM3 uncorrected for matrix elements and final state effects (c), and using density functional theory (d). The insert is a schematic of the lowest unoccupied molecular orbital.

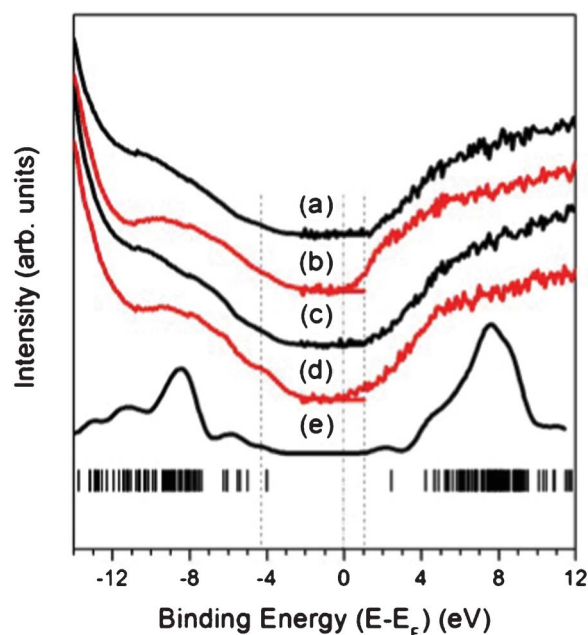


Fig. 4 Comparison of the combined photoemission and inverse photoemission spectra of molecular films of zwitterion **4** on graphene on copper (a,b) and on gold (c,d), along with the calculated density of states by PM3 (e) : (a) thick molecular film on graphene; (b) thin (1–2 nm thick) molecular film on graphene; (c) thick molecular film deposited on Au; (d) thin (1–2 nm thick) molecular film on gold.

state calculations based on a smaller highest occupied molecular orbital (HOMO) to lowest unoccupied molecular orbital (LUMO) gap that would be something like a combination of the semiempirical PM3 and density functional theory calculations (Fig. 2b).⁴ This is in general consistent with the expectation that zwitterions **1** and **3** both interact weakly with graphene compared to gold.⁴ The extent of adsorbate molecule to substrate interaction does matter: if the interactions of the molecular adsorbate with the substrate are too weak, then intermolecular interactions may dominate. When the intermolecular interactions are much stronger than the molecule-substrate interactions, then “wetting” of the substrate with the adsorbate layer is less likely to be energetically favorable. In that case, as long as there is little kinetic hindrance, *i.e.* diffusion of molecules across the surface is possible, then a Volmer–Weber island growth mechanism of the molecular film should be expected.

For the TCNQH-functionalized zwitterion **4**, the HOMO (highest occupied orbital) to LUMO gap and the general electronic structure derived from the combined photoemission and inverse photoemission spectra show little difference between adsorption on gold and graphene (Fig. 4). The related similarity of the electronic structure of the zwitterion **4** adsorbed at low molecular coverage on these substrates indicates that the interactions between such a molecule and these substrates should be equivalent or negligible. For both gold and graphene substrates, the LUMO edge is placed closer to the Fermi level when increasing the molecular film coverage.

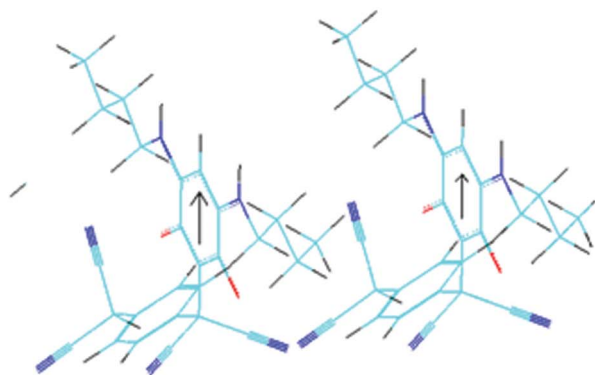
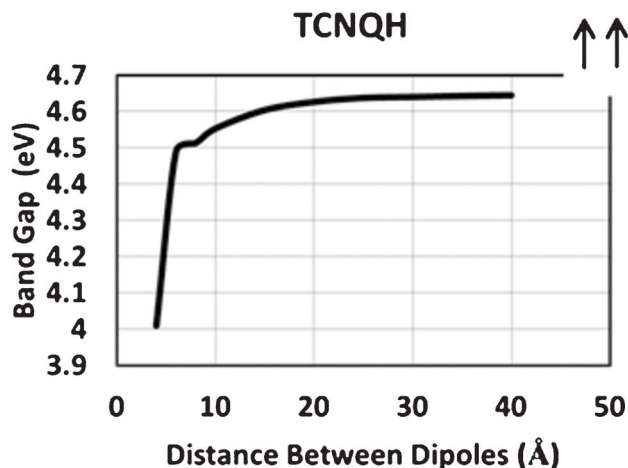


Fig. 5 Comparison of the HOMO–LUMO gap as a function of intermolecular spacing for a pair of TCNQ-derived *p*-benzoquinonemonoimine zwitterions (**4**) (the cif file of the crystal structure of **4** is available from CCDC 830133).⁴⁶ A number of different molecular orientations lead to the same qualitative result: the HOMO–LUMO gap decreases with decreasing intermolecular spacing.

This is accompanied by a decrease of the HOMO–LUMO gap, at variance with observations made with zwitterion **1**.⁴

Strong intermolecular interactions between molecules of **4** are consistent with the measured decrease of the HOMO–LUMO gap with increasing molecular film coverage. Model pairwise calculations on **4**, as a function of intermolecular distance, typically show a decrease in the HOMO–LUMO gap energies, as indicated in Fig. 5. This is just representative of the pairwise interactions: a number of different pair calculations were performed varying both polar and azimuthal angles and similar results were obtained for a number of different orientations. Indeed the decrease in the HOMO–LUMO gap is characteristic of a *p*-benzoquinonemonoimine zwitterion with intermolecular interactions sufficiently strong to support band dispersion, as previously observed with the zwitterion (6*Z*)-4-(benzylamino)-6-(benzyliminio)-3-oxocyclohexa-1,4-dien-1-olate, of formula $C_6H_2(=NHCH_2C_6H_5)_2(=O)_2$,^{2,3} schematically shown as **2** in Fig. 1.

While TCNQ is considered to be an electron acceptor molecule,^{30–39} the XPS spectra surprisingly indicate that the substrate Au 4f binding energies decrease by 200–300 meV upon adsorption of zwitterion **4** on gold (Fig. 6a), which is

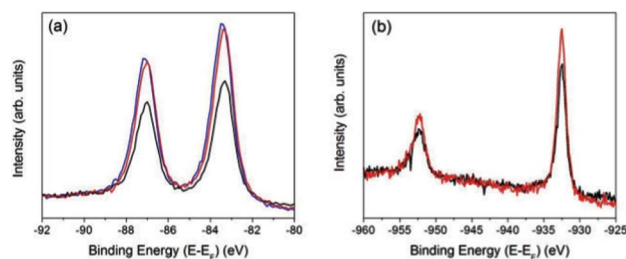


Fig. 6 The attenuation of the X-ray photoemission substrate signal from the (a) gold (Au 4f core levels) and (b) graphene on copper (the Cu 3p core levels) substrates. The core level spectra are shown for clean gold (blue), and the substrates following adsorption of 1 to 2 molecular monolayers of zwitterion **4** on gold (a) and graphene on copper (b) (shown in red). Much thicker molecular films create islands of zwitterion **4** molecules (Fig. 5) but do not suppress more than 15–30% of the substrate X-ray photoemission signal (black).

indicative of charge donation to the gold surface. This charge transfer is consistent with the CN groups donating electron density to gold. This is not expected for TCNQ,^{38,39} although negligible charge transfer between weakly bound TCNQ to Au(111) has been noted.³² Indeed for TCNQ adsorption on Cu(111), the Cu 2p core level binding energy increases.³³ While model calculations suggest that both TCNE (tetracyanoethylene) and TCNQ would in fact donate electron charge to graphene,^{34,35} *i.e.* n-type doping, in fact experiment provide evidence that p-type doping occurs.³⁸ Given that gold tends to be an electron acceptor in close proximity to graphene,^{49–51} electron donation from the TCNQ-derived moiety of **4** to Au(111) appears very plausible if electron donation to graphene occurs. Note that the electron-acceptor C=C double bond of TCNQ is no longer present in the TCNQH moiety of **4**. This, together with the possible loss of the hydrogen of the $C(CN)_2-H$ group upon adsorption of the molecule could explain the donor-type behaviour of zwitterion **4**.

The graphene on copper substrate core level photoemission data presented here (Fig. 6b) do not provide evidence for charge donation from the adsorbed zwitterion **4** molecules. Note, however, that the copper substrate is just a support for the graphene and thus different from the gold case. Charge transfer shifts due to the adsorption of the TCNQH moiety of **4** should be significant for graphene, but not be so substantial the copper substrate underneath. It is not just gold (as just noted) but also copper that tends to be an electron acceptor in close proximity to graphene.^{49–51} Therefore, an accurate assessment of the charge transfer from the adsorbed zwitterion **4** to the graphene is difficult as there could also be a charge transfer to the copper substrate. It is clear that an overall estimate of the charge transfer to the graphene from the adsorbed zwitterion **4** is technically more challenging to determine without taking a band mapping of the graphene layer. Furthermore, any charge donation caused by zwitterion adsorption may not be sufficient to perturb the substrate copper below the graphene. To the best of our knowledge, there are no studies concerning the adsorption of TCNQH₂ molecules on graphene. While it seems clear that TCNQ would

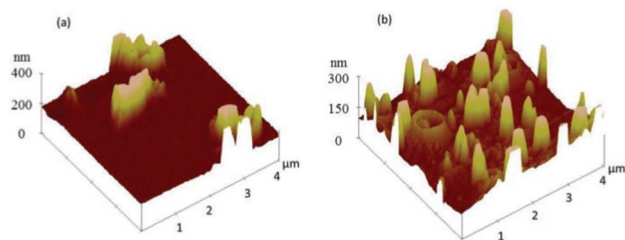


Fig. 7 Atomic force microscopy (AFM) images of the thicker molecular films of **4** (a) on gold and (b) graphene. The molecular thin film roughness are about 200 nm and 150 nm, respectively, while the roughness of the substrates are below 20 nm.

withdraw electron density from graphene,^{38,39} this does not prevent the TCNQH-functionalized zwitterion **4** from donating electron charge to the graphene.

Island growth of the zwitterion **4** on both gold and graphene on copper is apparent from the AFM images (Fig. 7). The clear tendency for these molecules to form clusters or islands results from intermolecular interactions that are far stronger than those with the graphene or gold substrates. We shall come back to this point later. The observed islands of 200 nm (on gold) and 150 nm (on graphene) in height do not obscure the substrates gold or copper X-ray photoemission core level signals (Fig. 6). The fact that the core level shift is uniform suggests that the TCNQH-functionalized zwitterion **4** on gold does cover the surface at low coverage and then adopts island growth at high coverage. This suggests a Stranski–Krastanov^{52,53} rather than a strict Volmer–Weber growth mode.⁵³ The critical layer thickness at the onset of island formation cannot be ascertained from our measurements here, but the very large substrate signal evident in the XPS data is indicative of the formation of a very thin (1–3 nm) molecular overlayer before island growth is initiated.

The crystal packing of the TCNQ-derived *p*-benzoquinone-monoimine zwitterion **4**, first described in prior work,^{46–48} presents multiple opportunities for strong hydrogen bonding, as illustrated in Fig. 8. Head-to-tail arrangement of two adjacent molecules is favored (Fig. 8a), as expected from dipolar electrostatic interactions and as observed with most members of the family of functionalized zwitterions. The TCNQH group provides additional possibilities for intermolecular hydrogen bonding with one proton of the butyl pending group (Fig. 8b). There are also hydrogen bonding interactions between the CN groups and aromatic protons of the TCNQH moieties of adjacent molecules (Fig. 8c). Such a wealth of hydrogen bonding should lead to intermolecular interactions stronger than commonly found with the non-functionalized quinonoid zwitterions and contribute to the type of molecular film growth seen here.

Conclusion

When deposited on graphene or gold, the TCNQH-functionalized *p*-benzoquinone-monoimine zwitterion **4** favors an island

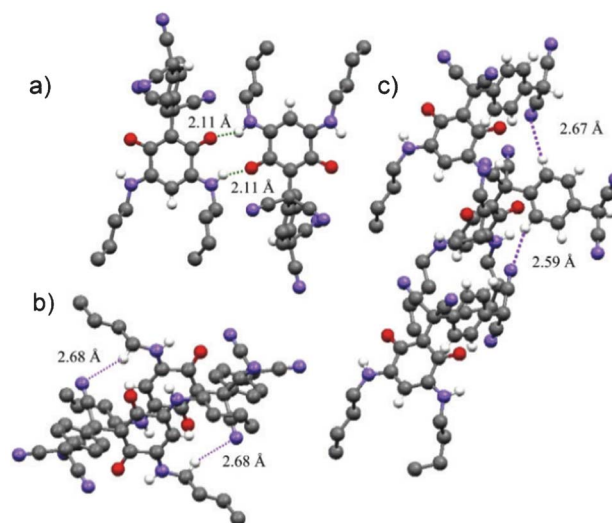


Fig. 8 Different views of the crystal packing of the TCNQ-derived *p*-benzoquinone-monoimine zwitterion **4**.⁴⁶ (The cif file of the crystal structure of **4** is available from CCDC 830133.) Some of the key hydrogen bonding interactions are indicated. Oxygen is shown in red, nitrogen in purple. Most hydrogen atoms (white) are not shown for simplicity, except when relevant.

growth morphology. The electronic structure seen in photoemission and inverse photoemission reveals limited molecule-substrate interactions and suggests strong intermolecular interactions. The latter are consistent with the known crystal-line structure of **4**, which reveals more hydrogen bonding interactions than for other quinonoid zwitterions previously investigated. The XPS studies of adsorption on gold favor a model of very thin initial molecular thin film coverage, prior to island growth, *i.e.* of Stranski–Krastanov growth type.

Acknowledgements

This work was supported by the Semiconductor Research Corporation, Division of Nanomanufacturing Sciences, Task ID 2123.001 (administered by Dan Herr), National Science Foundation through grants CHE-0909580, NSF-MRI 0923021 and PHY-1005071 as well as the Nebraska MRSEC (DMR-0820521), the Centre National de la Recherche Scientifique and the Ministère de l'Enseignement Supérieur et de la Recherche, the ANR (07-BLAN-0274-04 and ANR 2011-IS10-003-02), and by Basic Science Research Program through the National Research Foundation of Korea (NRF) funded by the Ministry of Education, Science and Technology (2010-0005706).

References

- J. Xiao, Z. Zhang, D. Wu, L. Routaboul, P. Braunstein, B. Doudin, Y. B. Losovyj, O. Kizilkaya, L. G. Rosa, C. N. Borca, A. Gruverman and P. A. Dowben, *Phys. Chem. Chem. Phys.*, 2010, **12**, 10329–10340.

- 2 L. Routaboul, P. Braunstein, J. Xiao, Z. Zhang, P. A. Dowben, G. Dalmas, V. DaCosta, O. Félix, G. Decher, L. G. Rosa and B. Doudin, *J. Am. Chem. Soc.*, 2012, **134**, 8494–8506.
- 3 L. G. Rosa, J. Velev, Z. Zhang, J. Alvira, O. Vega, G. Diaz, L. Routaboul, P. Braunstein, B. Doudin, Y. B. Losovjy and P. A. Dowben, *Phys. Status Solidi B*, 2012, **249**, 1571–1576.
- 4 L. Kong, G. J. Perez Medina, J. A. Colón Santana, F. Wong, M. Bonilla, D. A. Colón Amill, L. G. Rosa, L. Routaboul, P. Braunstein, B. Doudin, Chang-Mook Lee, Jaewu Choi, Jie Xiao and P. A. Dowben, *Carbon*, 2012, **50**, 1981–1986.
- 5 Y. Fang, N. Phuong, O. Ivasenko, M. P. Aviles, E. Kebede, M. S. Askari, X. Ottenwaelder, U. Ziener, O. Siri and L. A. Cuccia, *Chem. Commun.*, 2011, **47**, 11255–11257.
- 6 P. A. Dowben, D. Kunkel, A. Enders, L. G. Rosa, L. Routaboul, B. Doudin and P. Braunstein, *Topics in Catalysis (2013)*, in press.
- 7 D. A. Kunkel, S. Simpson, J. Nitz, G. A. Rojas, E. Zurek, L. Routaboul, B. Doudin, P. Braunstein, P. A. Dowben and A. Enders, *Chem. Commun.*, 2012, **48**, 7143–7145.
- 8 S. U. Son, J. A. Reingold, G. B. Carpenter, P. T. Czech and D. A. Sweigart, *Organometallics*, 2006, **25**, 5276–5285.
- 9 M. D. Ward, in *Struct. Bonding*, Springer-Verlag, Berlin, 2009, vol. 132, pp. 1–23.
- 10 A. Patra and T. P. Radhakrishnan, *Chem.–Eur. J.*, 2009, **15**, 2792–2800.
- 11 P. Krysiński, *Adv. Mater. Opt. Electron.*, 1998, **8**, 121–128.
- 12 R. M. Metzger, *Chem. Rev.*, 2003, **103**, 3803–3834.
- 13 B. F. Abrahams, R. W. Elliott, T. A. Hudson and R. Robson, *CrystEngComm*, 2012, **14**, 351–354.
- 14 T.-C. Tseng, N. Abdurakhmanova, S. Stepanow and K. Kern, *J. Phys. Chem. C*, 2011, **115**, 10211–10217.
- 15 N. Abdurakhmanova, A. Floris, T.-C. Tseng, A. Comisso, S. Stepanow, A. De Vita and K. Kern, *Nat. Commun.*, 2012, **3**, 940.
- 16 N. Abdurakhmanova, T.-C. Tseng, A. Langner, C. S. Kley, V. Sessi, S. Stepanow and K. Kern, *Phys. Rev. Lett.*, 2013, **110**, 027202.
- 17 Y. Yuan, P. Sharma, Z. Xiao, S. Poddar, A. Gruverman, S. Ducharme and J. Huang, *Energy Environ. Sci.*, 2012, **5**, 8558.
- 18 H. Aarnio, P. Sehati, S. Braun, M. Nyman, M. P. de Jong de, M. Fahlman and R. Österbacka, *Adv. Energy Mater.*, 2011, **1**, 792–797.
- 19 B. Yang, Y. Yuan, P. Sharma, S. Poddar, R. Korlacki, S. Ducharme, A. Gruverman, R. Saraf and J. Huang, *Adv. Mater.*, 2012, **24**, 1455–60.
- 20 Y. Yuan, T. J. Reece, P. Sharma, S. Poddar, S. Ducharme, A. Gruverman, Y. Yang and J. Huang, *Nat. Mater.*, 2011, **10**, 296–302.
- 21 P. W. Anderson, P. A. Lee and M. Saitoh, *Solid State Commun.*, 1973, **13**, 595–598.
- 22 J. R. Kirtley and J. Mannhart, *Nat. Mater.*, 2008, **7**, 520–521.
- 23 F. Zwick, D. Jérôme, G. Margaritondo, M. Onellion, J. Voit and M. Grioni, *Phys. Rev. Lett.*, 1998, **81**, 2974–2977.
- 24 F. Zwick, M. Grioni, M. Onellion, L. K. Montgomery and G. Margaritondo, *Phys. B*, 1999, **265**, 160–163.
- 25 F. Zwick, H. Berger, M. Grioni, G. Margaritondo and M. Onellion, *J. Phys. IV France*, 1999, **9**, 347–350.
- 26 D. Jérôme and H. J. Schulz, *Adv. Phys.*, 1982, **31**, 299–490.
- 27 S. A. Brazovskii, *The Physics of Organic Superconductors and Conductors*, Springer Series in Materials Science, Berlin, 2008, vol. 110, pp. 313–355.
- 28 F. Zwick, M. Grioni, G. Margaritondo, V. Vescoli, L. Degiorgi, B. Alavi and G. Gruner, *Solid State Commun.*, 1999, **113**, 179–184.
- 29 F. Zwick, S. Brown, G. Margaritondo, C. Merlic, M. Onellion, J. Voit and M. Grioni, *Phys. Rev. Lett.*, 1997, **79**, 3982–3985.
- 30 C.-L. Hsu, C.-T. Lin, J.-H. Huang, C.-W. Chu, K.-H. Wei and L.-J. Li, *ACS Nano*, 2012, **6**, 5031–9.
- 31 S. Barja, M. Garnica, J. J. Hinarejos, A. L. V. de Parga, N. Martín and R. Miranda, *Chem. Commun.*, 2010, **46**, 8198–8200.
- 32 I. F. Torrente, K. J. Franke and J. I. Pascual, *Int. J. Mass Spectrom.*, 2008, **277**, 269–273.
- 33 T. Patterson, J. Pankow and N. R. Armstrong, *Langmuir*, 1991, **7**, 3160–3166.
- 34 A. K. Manna and S. K. Pati, *Chem.–Asian J.*, 2009, **4**, 855–860.
- 35 M. Chi and Y.-P. Zhao, *Comput. Mater. Sci.*, 2012, **56**, 79–84.
- 36 D. C. Elias, R. R. Nair, T. M. G. Mohiuddin, S. V. Morozov, P. Blake, M. P. Halsall, A. C. Ferrari, D. W. Boukhvalov, M. I. Katsnelson and A. K. Geim, *Science*, 2009, **323**, 610–613.
- 37 R. Otero, J. M. Gallego, A. L. V. de Parga, N. Martín and R. Miranda, *Adv. Mater.*, 2011, **23**, 5148–5176.
- 38 Y. Qi, U. Mazur and K. W. Hipps, *RSC Adv.*, 2012, **2**, 10579.
- 39 J. I. Martínez, E. Abad, F. Flores and J. Ortega, *Phys. Status Solidi B*, 2011, **248**, 2044–2049.
- 40 C. Coletti, C. Riedl, D. S. Lee, B. Krauss, L. Patthey, K. Von Klitzing, J. H. Smet and U. Starke, *Phys. Rev. B: Condens. Matter Mater. Phys.*, 2010, **81**, 235401.
- 41 W. Chen, S. Chen, D. C. Qi, X. Y. Gao and A. T. S. Wee, *J. Am. Chem. Soc.*, 2007, **129**, 10418–22.
- 42 X. Wang, J.-B. Xu, W. Xie and J. Du, *J. Phys. Chem. C*, 2011, **115**, 7596–7602.
- 43 J. T. Sun, Y. H. Lu, W. Chen, Y. P. Feng and A. T. S. Wee, *Phys. Rev. B: Condens. Matter Mater. Phys.*, 2010, **81**, 155403.
- 44 Q.-Z. Yang, O. Siri and P. Braunstein, *Chem. Commun.*, 2005, 2660–2662.
- 45 Q.-Z. Yang, O. Siri, H. Brisset and P. Braunstein, *Tetrahedron Lett.*, 2006, **47**, 5727–5731.
- 46 T. Kauf and P. Braunstein, *Inorg. Chem.*, 2011, **50**, 11472–11480.
- 47 T. Kauf and P. Braunstein, *Dalton Trans.*, 2011, **40**, 9967–9970.
- 48 P. Braunstein, O. Siri, J.-p. Taquet and Q.-Z. Yang, *Angew. Chem., Int. Ed.*, 2006, **45**, 1393–1397.
- 49 I. N. Yakovkin, *Eur. Phys. J. B*, 2012, **85**, 1–8.
- 50 P. A. Khomyakov, G. Giovannetti, P. C. Rusu, G. Brocks, J. van den Brink and P. J. Kelly, *Phys. Rev. B: Condens. Matter Mater. Phys.*, 2009, **79**, 195425.
- 51 G. Giovannetti, P. A. Khomyakov, G. Brocks, V. M. Karpan, J. van den Brink and P. J. Kelly, *Phys. Rev. Lett.*, 2008, **101**, 26803.
- 52 I. N. Stranski and L. Krastanow, *Abhandlungen der Mathematisch-Naturwissenschaftlichen Klasse Iib. Akademie der Wissenschaften Wien*, 1938, **146**, 797–810.
- 53 E. Bauer, *Z. Kristallogr.*, 1958, **110**, 372–394.

Adsorption of TCNQH-functionalized quinonoid zwitterions on gold and graphene: evidence for dominant intermolecular interactions

Lingmei Kong, Lucie Routaboul, Pierre Braunstein, Hong-Gi Park, Jaewu Choi, John P. Colón Córdova, E. Vega, Luis G. Rosa, Bernard Doudine and Peter A. Dowben

The orbital energies with respect to the vacuum level using the semi-empirical PM3 model for

a) methoxybenzyl-functionalized zwitterion $C_6H_2(\dots NHR)_2(\dots O)_2$, where $R = -CH_2-C_6H_4-OCH_3$:

-0.38799 LUMO (+2)
-0.46374 LUMO (+1)
-2.11035 LUMO (0)
-7.57282 HOMO (0)
-9.01096 HOMO (-1)
-9.10518 HOMO (-2)

b) TCNQH-functionalization (TCNQH = $(NC)_2CC_6H_4CH(CN)_2$) of (6Z)-4-(butylamino)-6-(butyliminio)-3-oxocyclohexa-1,4-dien-1-olate $C_6H_2(\dots NHR)_2(\dots O)_2$ (where $R = n-C_4H_9$):

-0.54888 LUMO (+2)
-0.73256 LUMO (+1)
-3.736 LUMO (0)
-8.60307 HOMO (0)
-9.53232 HOMO (-1)
-9.65609 HOMO (-2)